

Dedicated to Professor Alexandru T. Balaban
on the occasion of his 85th anniversary

USING AN ALTERNATING MAGNETIC FIELD FOR COVERING A METALLIC STENT WITH A NEW MAGNETIC COMPOSITE

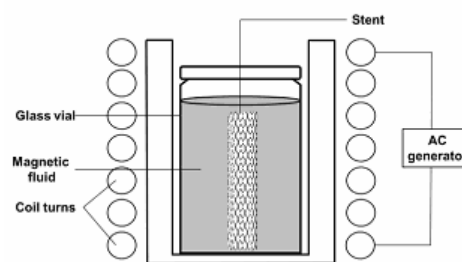
Aurica P. CHIRIAC,^{a,*} Loredana E. NITA,^a Liliana TARTAU,^b Iordana NEAMTU,^a
Nita TUDORACHI^a and Alina DIACONU^a

^a“Petru Poni” Institute of Macromolecular Chemistry 41-A Grigore Ghica Voda Alley, 700487 Iași, Roumania

^b“Gr. T. Popa” University of Medicine and Pharmacy, 16 University Street, 700115, Iași, Roumania

Received November 5, 2015

In the paper is presented the possibility of using the new magnetic composite (MC) (prepared *in situ* during functionalization of poly(maleic anhydride-co-3,9-divinyl-2,4,8,10-tetraoxaspiro [5.5] undecane) copolymer, by opening the anhydride ring with erythritol and by introducing magnetic nanoparticles into the polymer matrix) for covering the stent surface and improving the stent functionalities. The near infrared chemical imagistic NIR-CI analysis is used to investigate the spatial distribution of magnetite in the copolymer matrix while the acute toxicity investigation by calculating LD₅₀ allows the integration of MC in the group of low toxic substances. The covering of stent with MC is followed by optical microscopy and by the magnetization estimation.



INTRODUCTION

There is an increasing interest for superparamagnetic iron oxide nanoparticles (SPION) and their use for biomedical applications, in the context in which SPION have low toxicity and are suitable for *in vivo* applications as they are biodegradable, with the Fe product being recycled by cells.¹ Owing to magnetic nanoparticles (MNPs) dimensions and their magnetic properties, a close interaction with cells is possible as well the manipulation *in vivo* using an external magnetic field. More than that, the use of polymers for providing coatings with the desired properties, or functional groups for the attachment of specific

substances, allows tailoring the MNPs and enhances the potential for different applications through proper functionalization. By suitable selection, the functionalization ensures that magnetic nanoparticles are stable by suspending in the fluids and are as well chemically stable.²

Most of the functionalized magnetic nanoparticles used in biomedical applications require also rigorous surface functionalization to make the particles invisible to the reticulo-endothelial system of the body, and to prevent aggregation that would inhibit the transport of particles through the body. In this context, progress has been made in using iron oxide nanoparticles capped with dextran, polyethylene glycol,

* Corresponding author: achiriac1@yahoo.com

polyethylene oxide and other polymer coatings.³ Among biocompatible polymeric materials, both synthetic and natural polymers have been widely studied.⁴⁻¹⁶

In a previous paper was presented the synthesis of poly(maleic anhydride-co-3,9-divinyl-2,4,8,10-tetraoxaspiro [5.5] undecane), acquired through radical polymerization process.¹⁷ The aim was to prepare an alternant copolymer with precise placement of functional groups along the polymer backbones. The new structure owing to the suitable and specific functionalities is anticipated to be used as reactive polymer to link bioactive compounds via maleic anhydride moiety. The copolymer was improved in its functionality by maleic anhydride ring opening with different amounts of erythritol in order to confer antioxidant characteristics to the polymeric structure. The dual sensitivity of the polymeric structure, at temperature and pH was also demonstrated. The antioxidant character was evaluated by measuring the scavenger properties of the functionalized copolymer with erythritol against the 2,2-diphenyl-1-picrylhydrazyl radicals. The biocompatibility of the copolymer was also investigated by *in vivo* determination of the acute toxicity. Accordingly to value of the registered lethal dose (as being 50) and to the Hodge and Sterner toxicity scale, the polymer is included into the group of moderately toxic compounds. Further, a new magnetic hybrid composite is prepared, *in situ*, during the functionalization of poly(maleic anhydride-co-3,9-divinyl-2,4,8,10-tetraoxaspiro [5.5] undecane) copolymer, by opening the anhydride ring with erythritol and by introducing magnetic nanoparticles into the polymer matrix.¹⁸ The procedure allows for magnetic nanoparticles (MNPs) preparation. More than that, the new polymer matrix owing to its suitable and specific functionalities is anticipated to be used for further link of biological molecules *via* the maleic anhydride moiety and the polyol presence. The new hybrid composite is analyzed and the report of magnetization demonstrates that the prepared nanocomposites are superparamagnetic.

The market for stents is, in many ways, still emerging. While coronary stents are on the commercial market in one form or another for several years, the technologies and materials used to create the devices are improving every day.¹⁹ In addition, innovative technology is bringing new classes of devices (e.g., fully degradable stents) to market, technologies that grow the market and

even expand means of diagnosis and therapy stent to new patient populations in some cases. One of the most innovative aspects is the use of functionalized MNPs with antioxidative biomolecules deposited onto the stent surface to realize stent devices type for bio-requirements. Thus the new stent device will function as well as a delivery platform. At the same time, the prepared MNPs will represent a particularly appropriate tool based on their ability to be simultaneously functionalized and guided and/or removed by an external magnetic field owing to the magnetic NPs inclusion, meanwhile the presence of the antioxidative biomolecules would be the additional benefit.

In the paper is presented the possibility of using the new magnetic hybrid composite (prepared *in situ* during functionalization of poly(maleic anhydride-co-3,9-divinyl-2,4,8,10-tetraoxaspiro [5.5] undecane) copolymer, by opening the anhydride ring with erythritol and by introducing magnetic nanoparticles into the polymeric matrix) for covering the stent surface and improving the stent functionalities. This strategy allows for a combination of chemical modification and bringing antioxidant character of the stent surface. The procedure of the stent surface covering with the MC nanoparticles is performed in an alternating magnetic field (AMF). The magnetic hybrid nanocomposites, as stable colloidal suspensions composed of single-domain magnetic nanoparticles dispersed in appropriate solvent, can generate heat in the alternating magnetic field and create proper conditions for their uniform deposition onto the stent surface.

RESULTS AND DISCUSSION

In the designing of an appropriate architecture of an implanted medical device like a stent, quality control of these devices must be extremely high. Stent configuration, polymer structure and bioactive substance formula are important factors when a certain medical decision must be taken. With the addition of the polymer coating with encapsulated bioactive substance on stent, the uniformity and thickness of the coating must be ensured to guarantee proper bioactive substance delivery.¹⁹ Additionally, a critical function in terms of clinical complications is the acute toxicity expressed by advanced *in vitro* test, that must be monitored.

NIR-CI Examination

The near infrared chemical imaging (NIR-CI) is used to provide qualitative and quantitative analysis of localized and space-averaged chemical compositions. NIR-CI technique makes the fusion between near-infrared spectroscopy and image analysis and it is used in pharmaceutical applications to reveal the extent of the ingredient blending, particle size distribution, the presence of polymorphs, and the trace of contaminants. The method also visualizes the spatial distribution of the chemical compounds in a sample.²⁰⁻²³ NIR-CI, as a nondestructive technique, generates very large numbers (81,920) of spatially resolved NIR spectra in a few minutes. With the image analysis, RGB

(red-R, green-G and blue-B) images are created from the data that originated from the image pixels of the studied structures (pure polymers and the mixture between them at different ratio), as is presented in Fig. 1.

The only matrix that is not rescaled is the original data for imported, RGB image files. It can be observed the good distribution of the magnetite in MC (Fig. 1). NIR spectra in the 1200–2400 nm region of the neat polymeric matrix, magnetite and the magnetic composite are also presented in Fig. 1. MC presents characteristic NIR bands for the components, respectively at 1200, 1400 and 1623 nm for copolymer and 1100, 1447, 1670 and 2284 nm for magnetite (see Fig. 1).

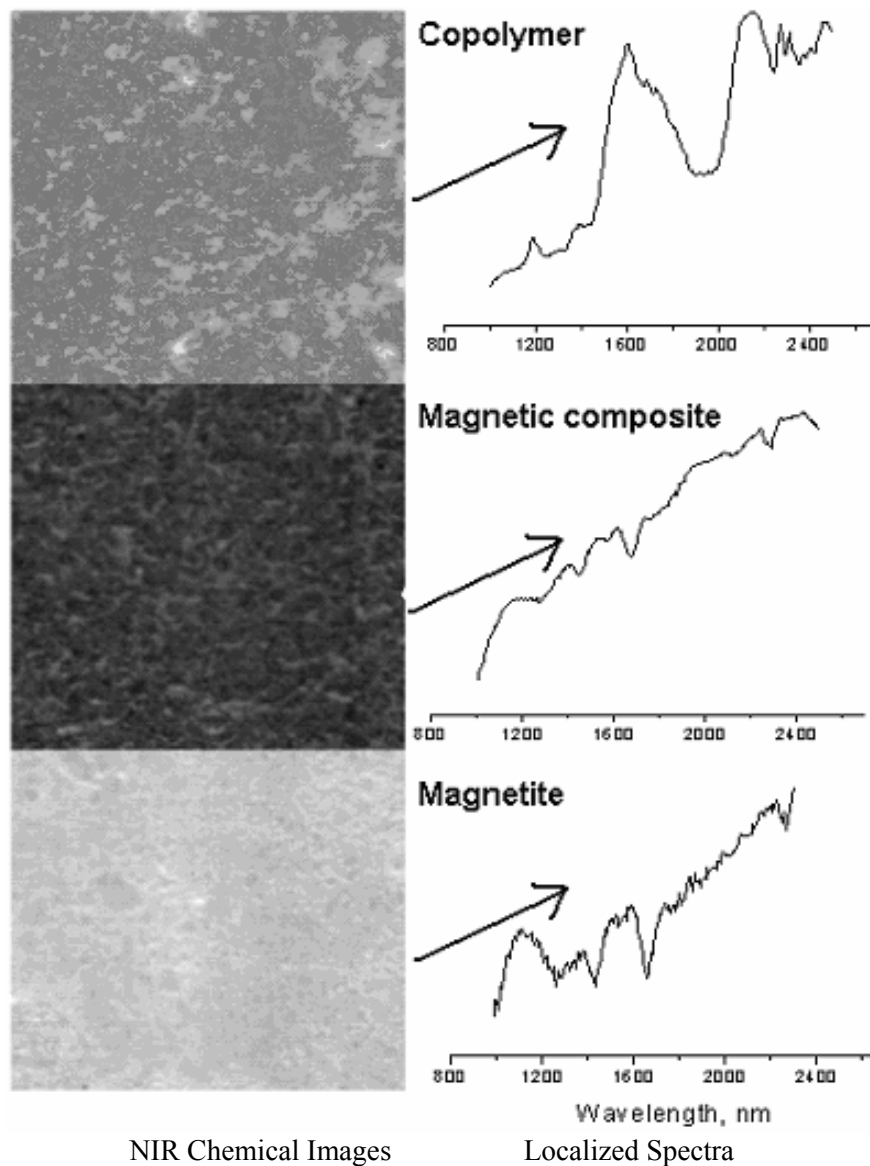


Fig. 1 – NIR-CI RGB images and NIR spectra of the copolymer matrix, magnetite and MC.

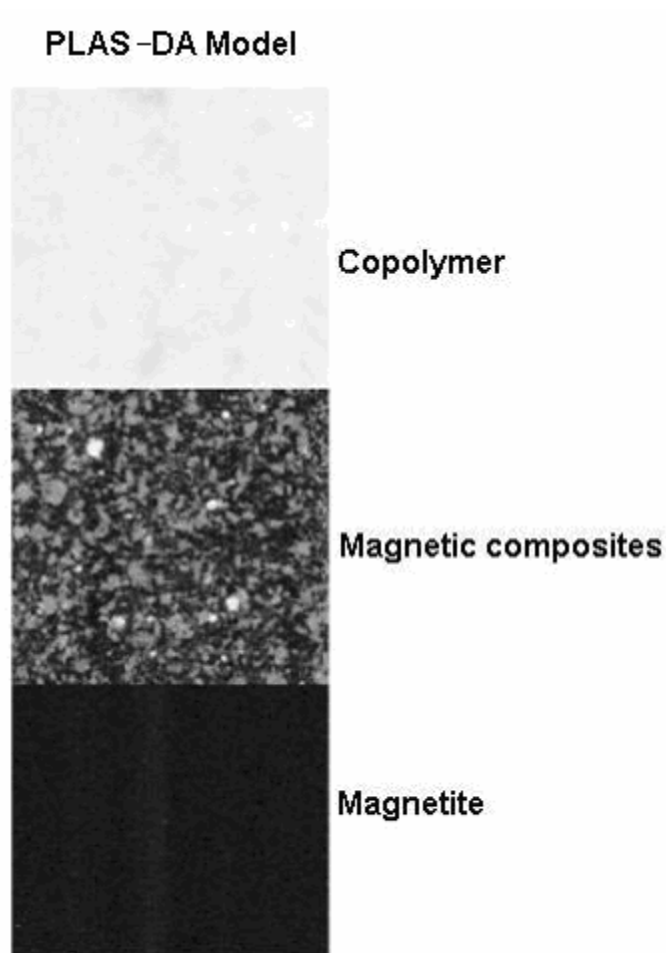


Fig. 2 – PLS-DA models for magnetic composite.

In order to obtain information about the spatial distribution of magnetite in copolymer matrix the PLS-DA model is used. With this model the data are decomposed into a small number of classification scores by utilization of information from both spectral variable and variable response. Fig. 2 presents the score images derived from magnetite component class. The codified pixel colour represents black for magnetite and light grey for the copolymer matrix. In case of MC sample the code colour in the most regions is grey, the intermediate colour between white and dark colours. These images, predominantly with grey score, evidence the homogeneous distribution of the magnetite into the polymeric matrix.

The acute toxicity investigation

The LD₅₀ value of the MC administered i.p. in a unique dose was estimated to be 2125 mg/kbw in mice (Fig. 3). The calculated LD₅₀ allows placing MC in the group of low toxic substances,

according to Hodge and Sterner toxicity scale. For biocompatibility investigation in mice, the dose of MC is 26.5 mg/kbw, representing 1/80 from LD₅₀.

There are no significant variations between the percentage values of blood leucocyte formula elements in mice treated with MC and in those with distilled water, 24 hours and 14 days in the experiment (Table 1).

Laboratory analysis does not show substantial differences of GOT, GPT and LDH activity, between group with MC and the control group, 24 hours and 14 days after MC administration (Table 2).

There are found no major variations of OC, PC and BC values, between the MC and control groups (Table 3).

There are not revealed significant pathological changes in the liver samples from animals treated with MC and with distilled water (Fig. 4).

The acute toxicity investigation demonstrates that the MC is relatively safe toxicologically when administered i.p. in mice. It is established that MC exercised similar modifications in leucocyte formula elements and in enzymatic activity with

distilled water, after i.p. injection in mice. The administration of MC does not modify the animal immune defense capacity, comparing with control group. There are observed no histopathological

modifications of the liver architecture in both MC and control groups. These results suggest a good *in vivo* biocompatibility of MC after systemic administration in mice.

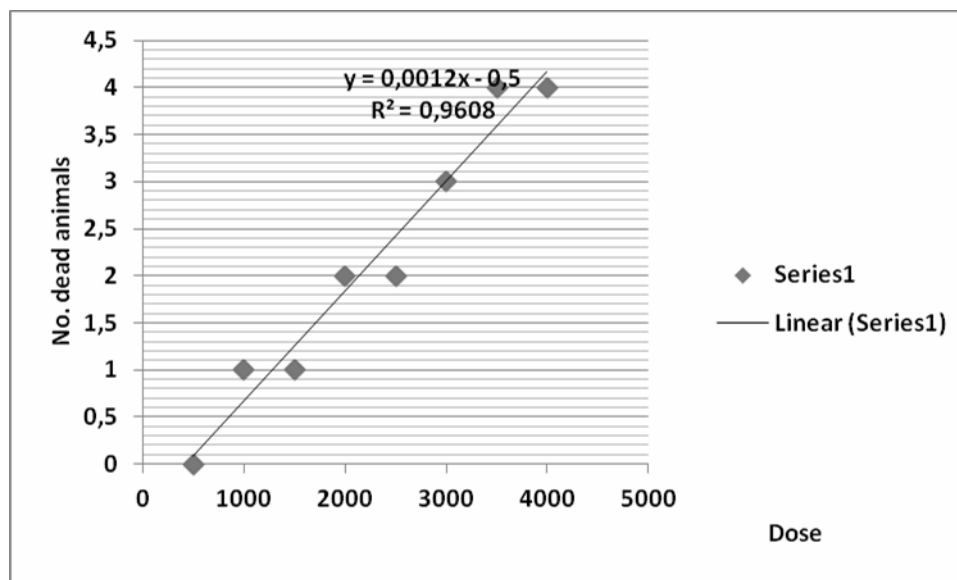


Fig. 3 – LD₅₀ of MC after i.p. administration in mice.

Table 1

Leukocyte formula animals treated with MC

		Leucocyte formula				
		% values				
		PMN	Ly	E	M	B
Distilled water	24 hrs	28.8±0.5	65.8±0.4	0.4±0.1	4.8±0.1	0.2±0.1
	14 days	28.5±0.2	66.2±0.3	0.6±0.05	4.5±0.2	0.2±0.1
MC	24 hrs	29.6±0.4	65.2±0.2	0.6±0.1	4.4±0.1	0.2±0.1
	14 days	29.5±0.2	64.9±0.3	0.7±0.05	4.7±0.2	0.2±0.05

Obs. Values were expressed as mean ± S.D; *p<0.05, **p<0.01 vs control for 6 mice.

Table 2

Glutamic pyruvic transaminase (GPT), glutamic oxaloacetic transaminase (GOT) and lactic dehydrogenase (LDH) activity in animals treated with MC

		GPT (U/mL)	GOT (U/mL)	LDH (U/L)
Distilled water	24 hrs	42.9±2,7	98.1±2,8	328.71±43.21
	14 days	43.2±2.3	98.7±4.1	336.37±27.39
MC	24 hrs	43.5±1,9	99.2±3,4	341.29±36.11
	14 days	44.8±3.5	99.5±1.7	344.23±37.42

Obs. Values were expressed as mean ± S.D. *p<0.05, **p<0.01 vs control for 6 mice.

Table 3

OC, PC and BC values in animals treated with MC

		OC (colonies/ml)	PC (colonies/ml)	BC (colonies/l)
Distilled water		803.27±45.39	517.43±62.19	725.29±54.26
MC		801.38±51.27	523.65±48.33	734.42±41.55

Obs. Values were expressed as mean ± S.D. *p<0.05, **p<0.01 vs control for 6 mice.

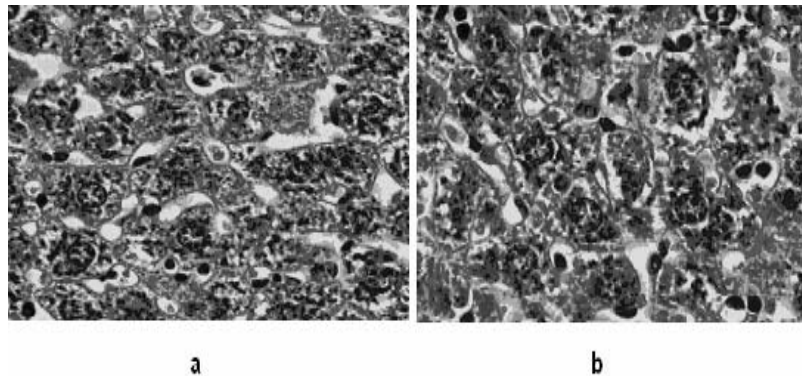


Fig. 4 – Liver architecture: a – normally in control animal; b - focal stasis, hepatic regeneration in animal treated with MC (Van Gieson coloration, x 40).

Optical microscopy and magnetic susceptibility analyses

Our MNPs are stable colloidal suspensions composed of single-domain magnetic nanoparticles dispersed in dioxane as appropriate solvent. The multifunctional characteristics of MNPs, and also their biocompatibility and low toxicity, make them great candidates as well for targeted drug delivery. Between other peculiar properties of the MNPs, one is that they generate heat in an alternating magnetic field, property which can be used for tumor hyperthermia, which takes advantage of higher sensitivity of tumor tissue to heat than normal tissue. At the same time, the magnetic nanoparticles can be excited in alternating magnetic field when is produced the up and down movement change. This movement promotes the dispersion of the magnetic nanoparticles, but also improves the stirring effect and the achieving of circulation to ensure the penetration and coupling

onto a metallic support for which the magnetic nanoparticles are presenting affinity.

Thus, this process to be able for efficiently coupling of MNPs onto the stent micro-surfaces, it is considered. The imaging by optical microscopy of the abluminal surface of the MC covered stent and also the magnetic susceptibility evaluation of the MC covered stent confirm the presence of the MNPs onto the stent surface.

Investigating the effects of alternating magnetic field on the deposition and distribution of the MNPs onto stent surfaces reveals the homogeneity and efficiency in filling the surface with the magnetic composite particles (Fig. 5 a and b; Table 4).

After MC deposition onto the stent surface which corresponds with an increase of weight by 25%, the magnetic susceptibility increased by 300 times. At the same time, after 5 repeated washings with distilled water the magnetic particles are kept on the stent, aspect confirmed by both optical microscopy (Fig. 5 b) and magnetic susceptibility value (Table 4).

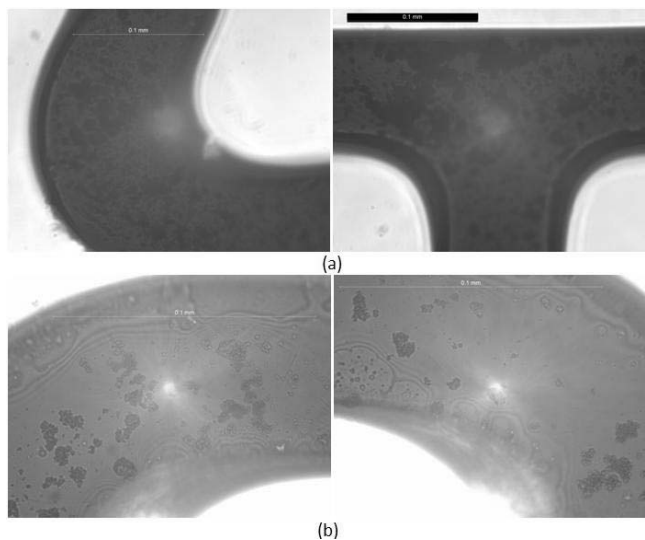


Fig. 5 – Images of stent after 4th cycles of MNPs deposition (a) and after washing 5 times (b). Magnification: 500x.

Table 4

Gravimetric and magnetic susceptibility analysis of the stents covered with MNPs

Cycle of deposition	Weight of stent, g		Magnetic susceptibility of stent, $e^4 V$	
	Before MNPs deposition	After MNPs deposition	Before MNPs deposition	After MNPs deposition
-	0.0120	-	0.023	-
First	-	0.0140	-	0.052
Second	-	0.0142	-	0.054
Third	-	0.0146	-	0.058
Fourth	-	0.0150	-	0.069
-	After washing 5 times			
-	-	0.0130	-	0.036

EXPERIMENTAL

Materials

All the reagents are of analytical purity and are used without further purification: 3,9-divinyl-2,4,8,10-tetraoxaspiro[5.5]undecane (U) (purity 98 %, Sigma-Aldrich), maleic anhydride (MA) (purity 95 %, Aldrich), 2,20-Azobis(2-methylpropionitrile) (AIBN) (purity 98 %, Sigma-Aldrich), 1,4-dioxane (purity 99.5 % Fluka), meso-Erythritol (E) (purity 99 %, Alfa Aesar), and diethyl ether (ACS reagent, anhydrous, purity 99.0 %, Sigma-Aldrich). Magnetite (Mg) is synthesized and supplied by R&D National Institute for Technical Physics (Iasi-Romania), dried powder sample with average particle size 220 nm by Dynamic Light Scattering. The water used in other experiments was purified using an Ultra Clear TWF UV System.

The stent platform 316L SS (annealed ASTM F138) from MEKO Laserstrahl- Material-Bearbeitung – Germany (Closed-cell, slotted-tube, 1.5 cm length, 13.7 mm thickness, 1mm stent strut) for the deposition of the MC, is used.

Polymer matrix synthesis

First P(MA-co-U) is realized through radical polymerization of monomers (in MA : U = 1 : 0.5 molar ratio) with radical initiator AIBN (2.92×10^{-4} M) in dioxane (22.5 %) at 75 °C, for 24 h. After cooling, the reaction mixture is added dropwise into diethyl ether and the copolymer is precipitated, washed with diethyl ether, isolated by filtration, and dried in a vacuum oven at room temperature and 600 mm Hg vacuum for 24 h.

Magnetic composite preparation technique

The magnetic composite MC is then *in situ* prepared by reacting 0.2 g copolymer matrix with 0.6 g E (P(MA-co-U)/E = 1/3 wt ratio) in 11 mL dioxane and in the presence of 5 wt % magnetite against copolymer amount (0.04 g magnetite powder D). The reaction is performed at 80 °C in dioxane, under stirring, for more than 6 h. During derivatization of MA with polyol E, anhydride ring is split and the magnetic compound is embedded and maintained into polymer network through physical bonds. After preparation, the magnetic composite is magnetically collected, thoroughly washed with ethanol, and further dried for 24 h at 25 °C and 600 mm Hg, in a vacuum oven.

Covering the metallic stent with MC

An alternant magnetic field (AMF of about $H = 200$ Oe, obtained from the solenoid with the following characteristics: $L = 700 \mu H$, $V = 125$ kHz, $I = 2.5$ A, $U = 1.3$ Kv, $P = 3$ Kvar) is used for the deposition of the NMPs onto the stent surface. The procedure consists in maintaining the stent in AMF for 10 min and around of 10 ml of NMPs dispersion of about 23.4 % concentration, with and $0.561e^{-4}$ volumetric magnetic susceptibility. The cycle of 10 min is repeated four times for the best deposition of NMPs onto stent surface. Note that the fifth deposition cycle has not brought improvements in the amount of deposited MC onto surface, nor in recorded value of the magnetic susceptibility of the stent. Fig. 6 illustrates the experimental setup for MNPs deposition onto the stent surface.

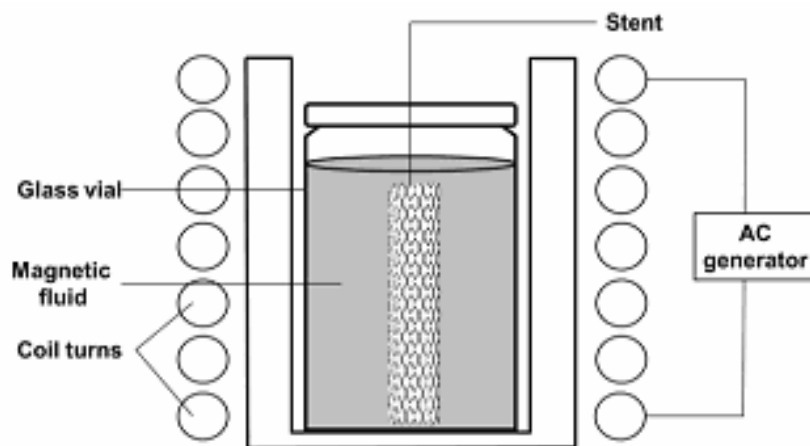


Fig. 6 – Experimental setup for MNPs deposition onto the stent surface.

After 10 min to maintain the particles in AMF, the reached temperature is about 52°C. It can conclude that these MNPs have relatively low Curie temperature points which lead to self-regulation and thus avoid overheating the tissue when excited by an AC magnetic field. Thus, these MNPs can be used for hyperthermia treatment, for example.

Methods of characterization

Chemical imaging on near infrared region with statistical analysis methods. Acquisition of optical and spectral data is carried with an integrated Chemical Imaging Workstation, provided by SPECIM Spectral Imaging Ltd (Finland). The optical data are collected with an ImSpector N17E imaging spectrograph for a resolution of each image of 320 X 640 pixels. The chemical images are taken with a NIR spectral camera, respectively an imaging spectrograph type ImSpector N17E at a rate of 60 – 350 Hz. The original image is recorded at a spatial resolution of 320x640 pixels and they are collected as a cube of data with two variable pixels (X and Y axis) and the third as absorbance variable (Z axis). The data is processed with EVINCE chemometric software package in order to explore the spectral and spatial information and classified and quantified image content.

Acute toxicity and in vivo biocompatibility of MC in mice. For the experiments white male Swiss mice (25-30g) are used. The animals are housed under standard laboratory conditions (relative humidity 55-65%, room temperature 23.0±2.0°C and 12 hours light: dark cycle). The acute toxicity of magnetic composite (MC) is assessed on the basis of median lethal dose (LD₅₀) calculation, using a limit dose test of “up and down” procedure at a limit dose of 5000 mg/kbw after a unique dose of MC intraperitoneal (i.p.) administration in mice.^{24,25}

It is determined the minimal dose that kills all the animals (LD₁₀₀) and the maximal dose that fails to kill any animal. Between these two limits, different dose at equal logarithmic intervals are chosen and administered in a group of five animals.²⁶ The mice are observed for 14 days, during which manifestations of toxicity (lack of appetite, depression, immobility, respiratory distress)²⁷ and mortality rates in each group are counted and the LD50 is calculated. It is used the arithmetical method Karber with the following formula:

$$LD_{50} = LD_{100} - \sum(axb)/n,$$

where: a - the difference between two successive doses of the substance administered, b - the average of the number of dead animals in two successive groups, n - the number of animals in a group.

The level of MC toxicity is evaluated according to the toxicity scale proposed by WHO/IPCS²⁸ adapted from the Hodge and Sterner scale.²⁹

The *in vivo* biocompatibility of MC is assessed by investigating of its influence on the leucocyte formula elements, biochemical and immune parameters, 24 hours and 14 days after a unique intraperitoneal (i.p.) injection in mice. After 14 days, serum opsonic capacity (OC), phagocytic capacity (PC) and bactericidal capacity (BC) of peritoneal macrophages are also determined. Liver fragments are collected for histopathological examination. The data are expressed as +/-SD (standard deviation) and analyzed using SPSS for Windows version 13.0 and ANOVA one way method. The study protocol is implemented according to recommendations of “Gr.T. Popa” University of Medicine and Pharmacy Ethical Committee for the Research, in compliance

with international ethical guidelines, regarding the experiments with animals.³⁰

Optical microscopy with Leica Microsystems Wetzlar GmbH Leica DM 2500. Optical microscopy images are acquired on a Reflected light brightfield microscope Leica DM 2500 (Leica Microsystems Wetzlar GmbH), magnification across the sample surface: 500x, with a 3.3 Mpix Leica DFC320 R2 digital camera (resolution 2088 x 1550 pixels) mounted on the trinocular head. The photo is later converted into digitized gray scale data for analysis.

Magnetic susceptibility with Magnetic susceptibility balance MSB – Auto (Geneq Inc.). The reading of volume susceptibility χ_v displayed by the balance is proportional to the sample's volume present in the measuring region of the balance.

CONCLUSIONS

The study is devoted to investigations made on poly(maleic anhydride -co-3,9-divinyl-2,4,8,10-tetraoxaspiro [5.5] undecane) copolymer functionalized with erythritol as matrix with encapsulated magnetite that is covered onto the abluminal metallic stent platform, with the aim of designing an appropriate architecture of an implanted medical device. The NIR-CI analysis reveals the uniform distribution of magnetite into the polymer matrix, while the acute toxicity investigation demonstrates that magnetic composite is relatively safe toxicologically and has a good *in vivo* biocompatibility after systemic administration in mice. The magnetic composite deposition on stent surface is confirmed by optical microscopy and magnetic susceptibility value.

Acknowledgements: This work was financially supported by the grant of the Roumanian National Authority for Scientific Research, CNCS-UEFISCDI, project number PN-II-211/2012 “Interdisciplinary research on multifunctional hybrid particles for biorequirements”. The authors thank Dr. Clemens Meyer-Kobbe from MEKO LASERSTRAHL-MATERIAL-BEARBEITUNG – Germany that has kindly provided us with stent samples for the experiments. The authors appreciate the colleagues and Prof. Horia Chiriac at the R&D National Institute for Technical Physics, Iași - Roumania for the expert assistance in manufacturing the magnetite sample.

REFERENCES

1. K.G. Neoh, L. Tan and E.T. Kang, “Nanomaterials for the Life Sciences”, Vol. 4, “Magnetic Nanomaterials”, WILEY-VCH Verlag GmbH & Co. KGaA, Weinheim, 2009.
2. V. K. Varadan, L. Chen and J. Xie, “Nanomedicine: design and applications of magnetic nanomaterials, nanosensors and nanosystems”, John Wiley & Sons, Ltd, 2008.
3. S. B. Darling and S. D. Bader, *J. Mater. Chem.*, **2005**, *15*, 4189–4195.

4. C. Hansi, A. Arab, A. Rzany, I. Ahrens, C. Bode and C. Hehrlein, *Catheter. Cardiovasc. Interv.*, **2009**, *73*, 488–496.
5. M. Haidopoulos, S. Turgeon, C. Sarra-Bournet, G. Laroche and D. Mantovani, *J. Mater. Sci. Mater. Med.*, **2006**, *17*, 647–657.
6. N. Faucheux, R. Schweiss, K. Lutzow, C. Werner and T. Groth, *Biomaterials*, **2004**, *25*, 2721–2730.
7. T. W. Chung, D. Z. Liu, S. Y. Wang and S. S. Wang, *Biomaterials*, **2003**, *24*, 4655–4661.
8. G. Mani, M. D. Feldman, D. Patel and C. M. Agrawal, *Biomaterials*, **2007**, *28*, 1689–1710.
9. T. Peng, P. Gibula, K. D. Yao and M. F. Goosen, *Biomaterials*, **1996**, *17*, 685–694.
10. O. F. Bertrand, R. Sipehia, R. Mongrain, J. Rodes, J. C. Tardif and L. Bilodeau, *J. Am. Coll. Cardiol.*, **1998**, *32*, 562–571.
11. C. C. Shih, C. M. Shih, Y. L. Chen, Y. Y. Su, J. S. Shih and C. F. Kwok, *J. Biomed. Mater. Res.*, **2001**, *57*, 200–207.
12. M. Uo, F. Watari, A. Yokoyama, Y. Matsuno and T. Kawasaki, *Biomaterials*, **2001**, *22*, 677–685.
13. M. L. W. Knetsch, Y. B. J. Aldenhoff and L. H. Koole, *Biomaterials*, **2006**, *27*, 2813–2819.
14. D. Lavigne, L. Guerrier, V. Gueguen, J. B. Michel, E. Boschetti and O. Meilhac, *Analyst*, **2010**, *135*, 503–511.
15. S. F. Long, S. Clarke, M. C. Davies, A. L. Lewis, G. W. Hanlon and A. W. Lloyd, *Biomaterials*, **2003**, *24*, 4115–4121.
16. J. M. Seeger, M. D. Ingegno, E. Bigatan, N. Klingman, D. Amery and C. Widenhouse, *J. Vasc. Surg.*, **1995**, *22*, 327–335.
17. A. P. Chiriac, L. E. Nita, N. Tudorachi, I. Neamtu, V. Balan and L. Tartau, *Mater. Sci. Eng. C.*, **2015**, *50*, 348–357.
18. I. Neamtu, A. P. Chiriac, L. E. Nita, N. Tudorachi and A. Diaconu, *J. Nanopart. Res.*, **2015**, *17*, 254–268.
19. I. Neamtu, A. P. Chiriac, A. Diaconu, L. E. Nita, V. Balan and M. T. Nistor, *Mini-Reviews in Medicinal Chemistry*, **2014**, *14*, 505–536.
20. G. Reich, *Adv. Drug Delivery Reviews*, **2005**, *57*, 1109–1143.
21. L. E. Nita and A. P. Chiriac, *J. Nanopart. Res.*, **2012**, *14*, 795–805.
22. E. W. Ciurczak and J. K. Drennen, (Eds.), “Pharmaceutical and Medical Applications of Near-Infrared Spectroscopy”, Marcel Dekker Inc., 2002, New York.
23. C. Rayn, E. Skibsted and R. Bro, *J. Pharm. Biomed. Analyses*, **2008**, *48*, 554–561.
24. E. Hodgson, “A Textbook of Modern Toxicology”, Wiley-Interscience, 3rd Edition, 2004.
25. *** OECD/OCDE guidelines 425 for testing of chemicals, acute oral toxicity-up-and-down-procedure(UDP) along with the conventional LD50 test and the fixed dose procedure (FDP), OECD test guidelines 420 and 423. Adopted 3rd October **2008**; cited from: http://asset.keepeek-cache.com/medias/domain21/_pdf/media424/69046-p88s0isiig/large/0.jpg
26. P. S. Deora, C. K. Mishra, P. Mavani, R. Asha, B. Shrivastava and K. N. Rajesh, *J. Chem. Pharm. Res.*, **2010**, *2*, 450–453.
27. K. R. Pritchett Corning, A. Girod, G. Avellaneda, P. E. Fritz, S. Chou and M. J. Brown, “Handbook of Clinical Signs in Rodents and Rabbits”, Charles River Laboratories, Wilmington, Mass, 2010.
28. *** *The WHO recommended classification of pesticides by hazard and guidelines to classification: 2009*.
29. A. C. Hodge and J. H. Sterner, *In toxicity's study: Some basic data*. (A.K. DONE) *Tempo Medical Afrique*, **1980**, 7.
30. *** *Protocole d'amendement à la convention européenne sur la protection des animaux vertébrés utilisés à des fins expérimentales ou à d'autres fins scientifiques*. Strasbourg; 22.06.1998.